Earth Planets Space, **53**, 207–212, 2001

Consequences of the neural network investigation for D_{st}-AL relationship

S. Kugblenu[1*], S. Taguchi[2], and T. Okuzawa[2]

[1]*Department of Electronic Engineering, University of Electro-Communications, Tokyo 182-8585, Japan*
[2]*Department of Information and Communication Engineering, University of Electro-Communications, Tokyo 182-8585, Japan*

(Received April 21, 2000; Revised November 24, 2000; Accepted January 17, 2001)

Several recent studies have suggested that most of the D_{st} main phase variations and of the AL variations similarly respond to a certain type of solar wind condition although the processes are independent of each other. This similarity suggests that some consistency between the D_{st} main phase development and AL variations exists, regardless of the existence of causality. In what situations this consistent relationship really exists or collapses has been examined with the technique of an Elman recurrent neural network. The network was trained with the D_{st} and hourly averaged AL indices for 70 storm events from 1967 to 1981, and tested for nine storms that occurred in 1982. The result shows that the D_{st}-AL relationship can be categorized into two types: high correlative mapping for which 80% and more of the D_{st} peak in the main phase is reproduced by AL, and partially correlative mapping where only about a half of the D_{st} peak is reproduced. It is found that whether the correlation is high or partial is determined by whether the D_{st} main phase develops smoothly or with a discontinuity, i.e., for storms having a discontinuity in the main phase, the coherency collapses. The discontinuity in the D_{st} main phase is associated with the rapid southward IMF change after the northward excursion. We suggest that it is this IMF variation to which storms and/or substorms respond in a highly complex manner and that such a complex response can be associated with about a half of the maximum ring current intensity.

1. Introduction

A geomagnetic storm is identified by the magnetic field depression on the Earth's surface. This depression is caused by the ring current flowing westward in the magnetosphere, and the strength of this ring current is generally monitored by the D_{st} index. During the D_{st} main phase intense substorms frequently occur, and this fact led to a view that the storm-time ring current is the result of a succession of substorm particle injections (Akasofu, 1968).

From this view point, Kamide and Fukushima (1971) attempted to model the storm-time D_{st} variations. By using the temporal evolution of the AL index which represents substorm activities, and by introducing an efficiency parameter which expresses the ring current growth relative to the substorm intensity, the authors successfully reproduced the D_{st} main phase variations.

As the solar wind data became available, there appeared another view in which the controlling factor of the main phase of magnetic storms is the interplanetary magnetic field (IMF) rather than substorm activities. Kokubun (1972) showed that the growth of D_{st} in the storm main phase is associated with sudden negative change in IMF B_z. Russell *et al.* (1974) found that a storm is triggered when the southward IMF B_z exceeds a threshold level. Using the solar wind velocity and density together with the southward B_z, Burton *et al.* (1975) successfully reproduced the temporal variation of the D_{st} although their model tends to deviates from the observation in the recovery phase. Clauer and McPherron (1980), and Clauer *et al.* (1983) showed that the response of the asymmetric disturbance of the mid-latitude geomagnetic field has better correlation with the southward B_z rather than the AL index, which suggests that storms are directly controlled by the southward B_z.

For a storm, is substorm occurrence really needed? Kamide (1992) attempted to answer this question, and suggested that substorm occurrence is not a necessary condition for a storm. This suggestion was quantitatively demonstrated by Iyemori and Rao (1996), who examined the one-minute time resolution D_{st} indices, which are referred to as *ASY*/*SYM*, and found that the H component of the *SYM* index does not show any development after substorm onset. This suggests that the substorm expansion is not needed for the storm development. Iyemori and Rao (1996) also showed that superposed *SYM* (H component) decays after substorm onset rather than develops, and implied that substorm is an energy dissipation process in the magnetosphere during a storm, not a process needed for the development of the storm-time ring current.

The result by Iyemori and Rao (1996) implies that the development of the storm-time ring current can be accurately modeled without any input of substorm activity such as the AL index. Such accurate models have been enabled by recent advances in linear/non-linear prediction filter (e.g., McPherron, 1997; Klimas *et al.*, 1998) and in artificial neural network (Wu and Lundstedt, 1997; Kugblenu *et al.*, 1999). In the linear prediction analysis McPherron (1997) showed that 85% of the D_{st} variance is accounted for by the solar

*Now at Ghana Telecom, Headquarters, Ghana.

wind dynamic pressure and a coupling function expressed by the solar wind speed, IMF B_z, and B_y. Klimas *et al.* (1998) constructed nonlinear analogues of VBs input and D_{st} output, and showed that the prediction performance of their model is better than that of the Burton's model. Wu and Lundstedt (1997) made an Elman recurrent neural network model for the D_{st} variations from IMF B_z and the solar wind number density and speed. Although discrepancy between the model and observation sometimes occurs in the recovery phase, and for the accurate reproduction of this recovery phase some arrangement may be needed (Kugblenu *et al.*, 1999), the model of Wu and Lundstedt (1997) showed a remarkably good performance; i.e., the correlation coefficient between the observed D_{st} and the modeled D_{st} is 0.91. Higher correlation coefficient has been reached by the neural network model by Kugblenu *et al.* (1999), who included three hourly D_{st} before the D_{st} minimum in the network training, and succeeded in accurate reproduction of the D_{st} decay in the recovery phase. It should be noted that a recent report by O'Brien and McPherron (2000) showed that for $D_{st} > -150$ nT the decay time of D_{st} in the recovery phase can be modeled by VBs without invoking D_{st} itself.

The AL index representing substorm activities has been also used as a prediction target, and reasonably good reproduction has been reported, for example, by McPherron (1997), and Gleisner and Lundstedt (1997). McPherron (1997) used the solar-wind coupling function that is the same as the one for the best D_{st} prediction, and showed that this function accounts for about 60% of the AL variance. More accurate reproduction was obtained by Gleisner and Lundstedt (1997), who showed that a neural network with the solar wind number density, speed, IMF B_y, and B_z can account for 76% of the AE index variance. It thus appears that most of the D_{st} and AL variations respond to similar solar wind condition although these responses may occur in a manner independent of each other.

This suggests that some consistency between the D_{st} and AL variations exists, regardless of the existence of causality. McPherron (1997) showed that about 70% of the D_{st} variance is accounted for by the AL index using the linear prediction filter. However, if the prediction for D_{st} and/or AL only from the solar wind conditions is not reasonable in some situations, consistency would not exist, unless D_{st} and AL are strongly coupled presumably in cause-and-effect relationships.

In this paper, we examine in what situations such consistent relationship exists or collapses by using an Elman recurrent neural networks (Elman, 1990). Our results show that the D_{st}-AL relationship can be categorized into high and partially correlative cases, and that whether the coherency between the observed D_{st} and the one mapped through the neural network is high or partial is determined by whether the D_{st} main phase develops smoothly or with a discontinuity. From this finding we consider the solar wind conditions to which D_{st} and/or AL do not respond in a predictable manner, and discuss storm-substorm relationships.

2. Approach

Techniques of artificial neural network (ANN) are input-output models which are efficient in capturing a nonlinear process as well as a linear process, and multi-layer ANN is considered to be a nonlinear function which maps a point in an m-dimensional input space into a point in an n-dimensional output data space. The general concept of the ANN is described for example in Hertz *et al.* (1991). Some of ANN techniques have been successful in predicting the D_{st} index from solar wind parameters (*see* review by Lundstedt, 1997). In particular, remarkably good reproduction of D_{st} was obtained with an Elman recurrent neural network by Wu and Lundstedt (1997).

Elman recurrent network is a class of multi-layer ANN's with a feedback loop from the hidden layer connected to the input layer (Elman, 1990). The general architecture for the Elman recurrent network is illustrated in Fig. 1. The recurrent connection from the hidden to the input layers allows the network to generate and detect time-varying patterns. The delay in this connection stores values from the previous time step, and these values are used in the current time step. Figure 1 shows that there are R true input units, S_1 hidden units, and S_2 output units. The input layer also has the context units besides the true input units. The context units have a one-to-one correspondence to the feedback connections from the hidden units, so that the number of the context units is the same as that of the hidden units. The context units simply act as a copy of the activations of the hidden units from the previous time step. The activation function is the hyperbolic tangent for the hidden layer, and linear for the output layer.

We designed the Elman ANN for which the hourly average AL index and the one-hour resolution D_{st} index are input and output, respectively. This is an architecture with a single input/output, that is, both R (the number of the input units in Fig. 1) and S_2 (the number of the output units) are unity. It should be noted that we do not assume in this architecture that AL for input is the cause of D_{st}. The number of the hidden units (S_1) was taken to be 13 because this gives the best correlation between the prediction and observation for a certain particular type of storms as is shown later.

The D_{st} index was obtained from the National Space Science Data Center OMNI database. For the AL index, whose 1-minute values are derived by the World Data Center C2 of Kyoto University, we used the hourly data from the database of World Data Center C1 of the Danish Meteorological Institute so that the input and output parameters can have the same time-resolution.

We examined the D_{st} data from 1967 to 1981 except for the intervals when the AL index are not available, and took 70 storm events with a D_{st} minimum of < -100 nT regardless of its duration and structure. We made training data sets of D_{st} and AL for these storm intervals, and these amounted to approximately 11,110 hours. For the training, the input unit was fed with the AL index, and the corresponding D_{st} index data were fed to the output unit. To test the trained network, only the AL index was fed to the input of the network. This testing was done for 9 storms with a D_{st} minimum of < -100 nT from 1982. Storm periods for 1983 and 1984 were used for a validation purpose of the network.

3. Results

In Fig. 2 we show examples for which the ANN can give high correlative mapping so that D_{st} is well reproduced by AL. Figure 2(a) is the storm of April 10–13, 1982 which has

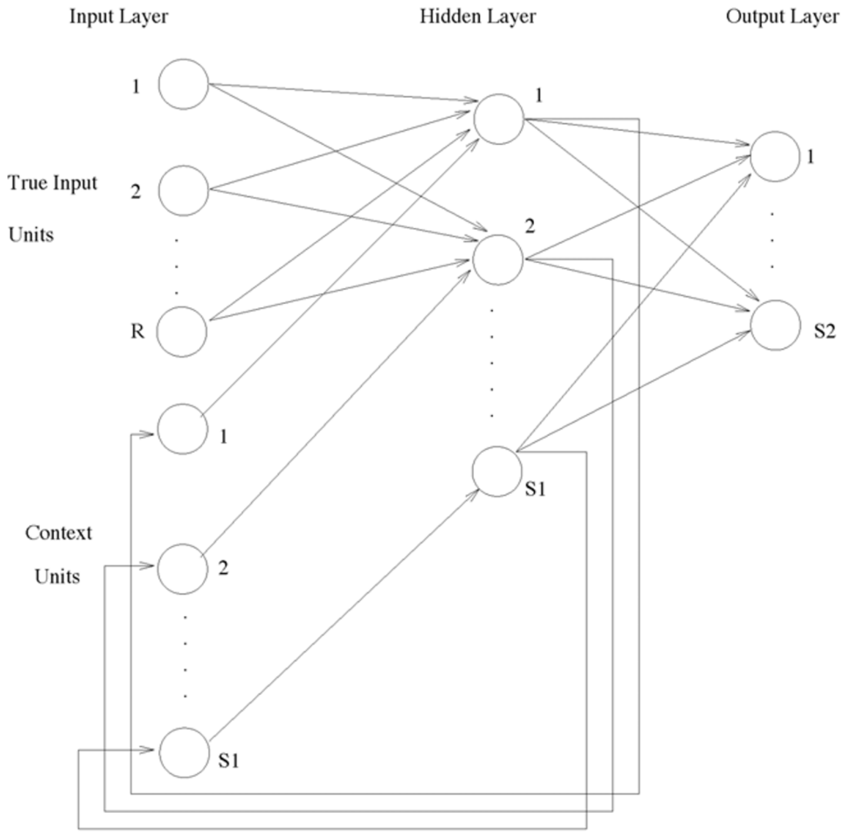

Fig. 1. Elman recurrent neural network architecture.

a minimum D_{st} of -137 nT. The hourly AL index used for the input are plotted in the top panel. In the bottom panel the solid line indicates the measured D_{st} values while the broken line represents prediction from AL. The horizontal axis represents the universal time. About 90% of the D_{st} peak magnitude is reproduced, and the recovery from the D_{st} peak is also well modeled. This represents that our ANN can successfully find some consistent relationship between the D_{st} and AL indices. Similar good reproduction can be seen in the storm of September 21–23, 1982 (Fig. 2(b)). For this case, almost 100% of the D_{st} peak is reproduced although the prediction peak occurs with a few hours delay.

Two examples for which ANN identifies only partial consistency are shown in Fig. 3. Figure 3(a) shows the storm event of July 13–16, 1982 during which D_{st} dropped rapidly to -160 nT in the beginning of the main phase, and then a small recovery (an increase in D_{st}) to a value of -133 nT occurred. This creates a discontinuity in the main phase. For this storm event, the modeled D_{st} reaches only -160 nT, i.e., about a half ($\sim$45%) of the peak value of the measured D_{st}, showing that the mapping between D_{st} and AL is partial and imperfect. The difference between the reproduced and measured D_{st} variations becomes small after the D_{st} minimum, and reasonably good reproduction starts at the beginning of the slower decaying stage of the recovery phase, i.e., about 10 hours after the D_{st} minimum peak.

Figure 3(b) shows the storm event of September 5–8, 1982. This storm event can be also seen to exhibit a discontinuity in the main phase. Similarly to the result for Fig. 3(a), only about a half of D_{st} minimum peak is reproduced. The imperfect reproduction continues during about 15 hours after the peak, i.e., before the start of the slower decaying part of the recovery phase. This is also similar to the result for Fig. 3(a).

Table 1. Prediction ratio for the test storm events. The test storm events which were selected from 1982 are shown in the second column. The third column represents the prediction ratio, i.e., the ratio of the predicted D_{st} minimum to the observed D_{st} minimum. This ratio is estimated with accuracy of 5%.

Event	Event date	% of prediction
(1)	March 2	45
(2)	September 22	100
(3)	September 6	55
(4)	November 24	55
(5)	April 10	90
(6)	July 14	45
(7)	September 26	60
(8)	November 22	80
(9)	August 7	100

We calculated the ratio of the predicted D_{st} minimum relative to the observed D_{st} minimum for the 9 test storm events (Table 1). The result shows that correlative mapping from AL to D_{st} for the 9 storms can be categorized into two types: high and partial. The high correlative mapping was defined as cases where 80% and more of the D_{st} peak in the main

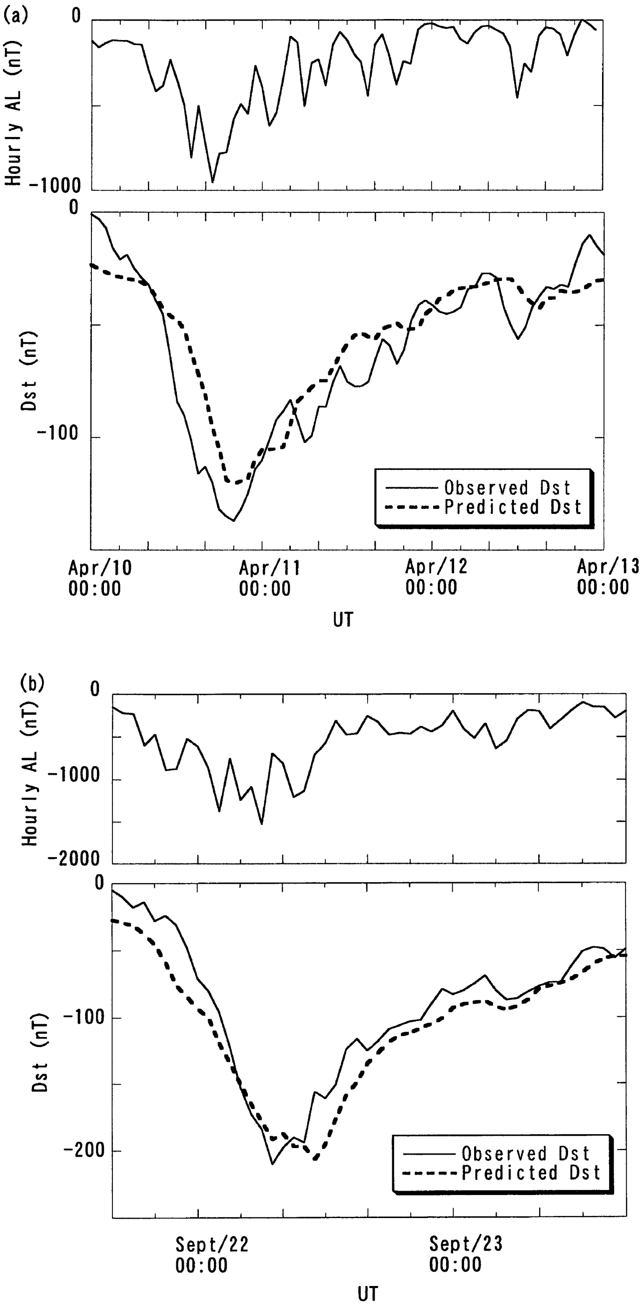

Fig. 2. Typical examples of high correlative mapping for which the D_{st} index (bottom) is well reproduced by the hourly average AL index (top).

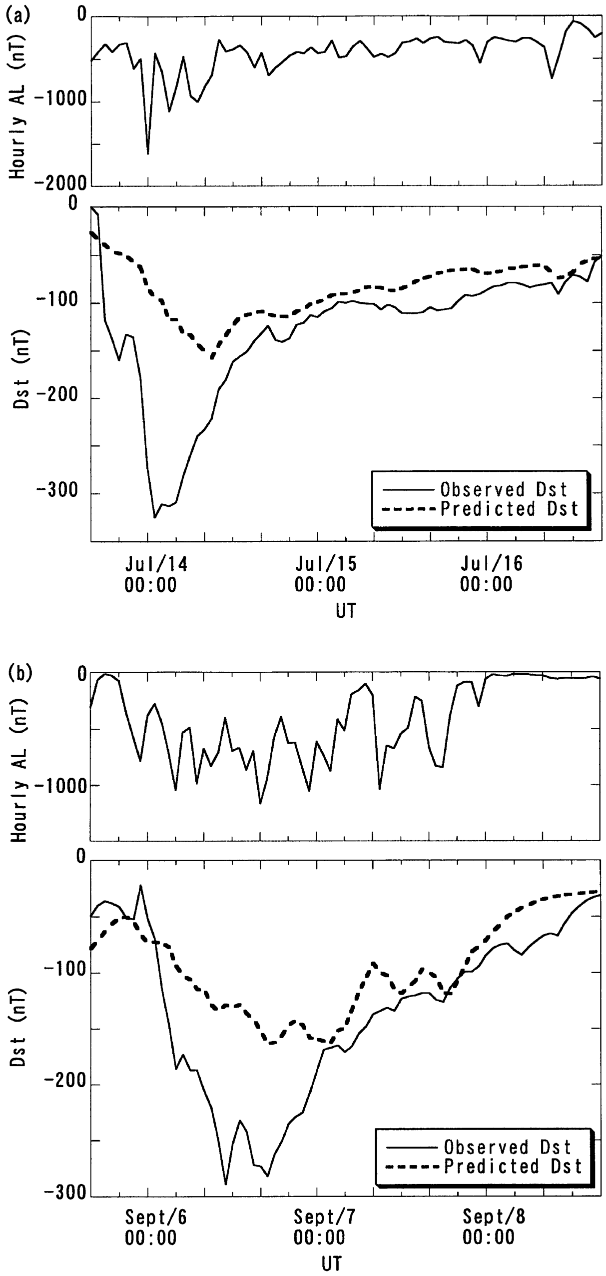

Fig. 3. Examples of partially correlative mapping. Format is the same as the one for Fig. 2.

phase can be reproduced, and four cases are in this category. The other five cases have prediction ratios of 45–60%, and are regarded as partially correlative mapping. The D_{st} variations for these five cases have a discontinuity in the main phase as can be seen in the Fig. 3 events.

4. Discussions and Conclusion

Using the technique of ANN, we have shown that there can exist some consistent D_{st}-AL relationships for one-step main phase storm. When we accept that the D_{st} variations can be accounted for by solar wind conditions without need for substorm expansion, the existence of consistency between D_{st} and AL would reflect that AL can be also reproduced by the solar wind condition, as has been shown in the results with the technique of linear prediction filters (McPherron, 1997) and of ANN (Gleisner and Lundstedt, 1997).

We believe that importance of our results lies in cases where consistent relationship collapses. This would represent that D_{st} and/or AL do not response to the solar wind in some coherent manner when the storms occur with a discontinuity in the D_{st} main phase. Storms with a discontinuity in the main phase may be regarded as a two-step growth in the main phase. This type of main phase growth has been recently examined by Kamide *et al.* (1998), who found that for more than 50% of intense storms, the main phase undergoes a two-step growth. Similar type of the D_{st} variations has been also referred to as an extended main phase, and examined in detail by Srivastava *et al.* (1999). Kamide *et al.* (1998) also clarified the solar wind condition for the two-step main phase growth; if a northward excursion occurs during southward B_z, and IMF turns southward again, it leads to a well-defined two-step growth in the storm main phase.

We have checked IMF data for our five test cases for the partial prediction (see Table 1). IMF data near the D_{st} discontinuity are available for only two cases of the five. One example (March 2, 1982 storm) is shown in Fig. 4. IMF B_Z, solar wind number density and speed are plotted together with the AL and D_{st} index. It is evident that a discontinuity of D_{st} in the main phase coincides with the rapid southward turning of IMF from the northward excursion. It is also seen that this IMF change is coincident with start of the discrepancy between the measured and modeled D_{st}. Coupled with the statistical result by Kamide *et al.* (1998) regarding the IMF condition, it is very likely that the rapid southward IMF turning after the northward excursion is responsible for the collapse of the predictable D_{st}-AL relation.

Figure 4 also shows that both solar wind number density and speed enhance roughly in coincident with the D_{st} discontinuity in the main phase. For two events other than this event, solar wind plasma data are also available, and one event has a similar enhancement in the number density near the D_{st} discontinuity, while in the other event such an enhancement is not seen. We cannot determine from our events if the number density enhancement is associated with the D_{st} discontinuity in the main phase. It should be noted that several reports have pointed out that the variations of the solar wind number density can affect the AL index (e.g., Tsurutani *et al.*, 1988; Shue and Kamide, 1998).

For the question of why the D_{st}-AL consistency collapses in coincidence with this type of IMF variations, we speculate the following scenario. The solar-wind controlled part of the D_{st} development would not quickly respond to this rapid southward turning. However, substorms can quickly respond and occur. These substorms may be more intense than the ones that occur in situations when there is no significant southward B_z before a northward excursion, because the southward B_z before the northward excursion may activate the magnetospheric state so that the next southward B_z can create more intense substorms. It can be seen in Fig. 4 that the AL index reaches larger negative values after the second southward B_z than in the interval corresponding to the first southward B_z. In correlation with this kind of second intense substorms the O^+ energy density in the inner magnetosphere would become high (Daglis *et al.*, 1994), and hence the accumulation of the O^+ population may cause further D_{st} development (Kamide *et al.*, 1998).

In this scenario, substorm activities are needed besides the solar wind to account for the D_{st} variations. If the substorm activities also have some consistent relationship with the solar wind condition, strong consistency between the D_{st} and AL variations might be identified. However, such consistency has not been identified in this study. This may imply that the level of substorm activities initialized by a rapid southward IMF turning is dependent on the activity level in the previous stage so that the reproduction of AL only from the current solar wind condition may be difficult (Vassiliadis *et al.*, 1995; Horton and Doxas, 1998). This may be also consistent with the statistical result by Kamide *et al.* (1998), who showed in their figure 4 that while southward B_z for the first and second development of D_{st} have similar magnitude, the corresponding AL takes a quite different magnitude. Hence, for storms having a discontinuity in the D_{st} main phase, AL would not have very high correlation with the solar wind conditions, and this is also true for D_{st} because the substorm activities represented by such AL can contribute to the D_{st} variations.

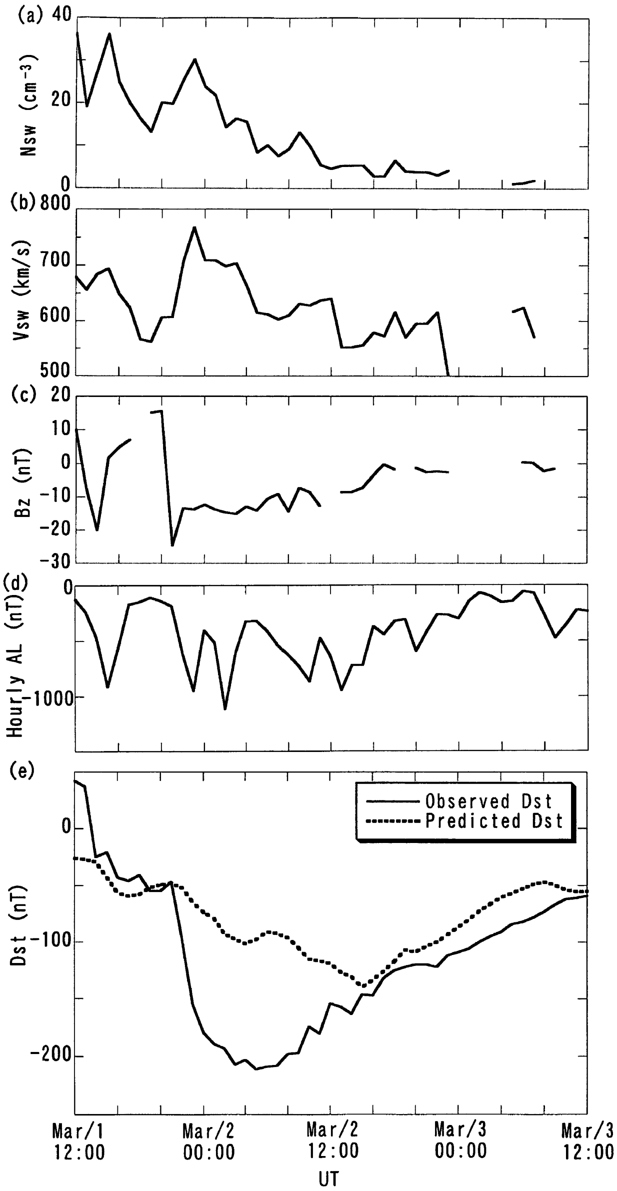

Fig. 4. Solar wind density, speed, the north-south component of IMF, and the corresponding AL (hourly average values) and D_{st} variations for the March 2, 1982 storm event. In the D_{st} plot, the solid line represents the variations of the D_{st} index showing a discontinuity in the main phase. The broken line shows D_{st} reproduced by the AL index.

In conclusion, using an Elman ANN, we have shown that while D_{st} and AL have some consistent relation for single-step main phase storm, such consistency collapses for the storms having a discontinuity in the main phase. The discontinuity in the D_{st} main phase is associated with the rapid southward IMF change after the northward excursion. We suggest that it is this kind of IMF variations to which storms and/or substorms do not respond in a predictable manner and that such a complex response can be associated with about a half of the maximum ring current intensity. We would like to stress that this suggestion comes from the situation where the neural network mapping fails. This may shed a new light on the use of neural networks for space physics phenomena in contrast to previous use in which better prediction has been aimed at.

Acknowledgments. Solar wind and IMF data were obtained from NSSDC/NASA. This study was partly supported by the joint research program of the Solar-Terrestrial Environment Laboratory, Nagoya University.

References

Akasofu, S.-I., *Polar and Magnetospheric Substorms*, 280 pp., D. Reidel Publ. Co., Dordrecht-Holland, 1968.

Burton, R. K., R. L. McPherron, and C. T. Russell, An empirical relationship between interplanetary conditions and D_{st}, *J. Geophys. Res.*, **80**, 4204–4214, 1975.

Clauer, C. R. and R. L. McPherron, The relative importance of the interplanetary electric field and magnetospheric substorms on the partial ring current development, *J. Geophys. Res.*, **85**, 6747–6759, 1980.

Clauer, C. R., R. L. McPherron, and C. Searls, Solar wind control of the low-latitude asymmetric magnetic disturbance field, *J. Geophys. Res.*, **88**, 2123–2130, 1983.

Daglis, I. A., S. Livi, E. T. Sarris, and B. Wilken, Energy density of ionospheric and solar wind origin ions in the near-Earth magnetotail during substorms, *J. Geophys. Res.*, **99**, 5691–5703, 1994.

Elman, J. L., Finding structure in time, *Cognitive Science*, **14**, 179–211, 1990.

Gleisner, H. and H. Lundstedt, Response of the auroral electrojets to the solar wind modeled with neural networks, *J. Geophys. Res.*, **102**, 14,269–14,278, 1997.

Hertz, J., A. Krogh, and R. G. Palmer, *Introduction to the Theory of Neural Computation*, Lecture Notes vol. 1, Santa Fe Institute Studies in the sciences of complexity, Addison-Wesley, Redwood City, 1991.

Horton, W. and I. Doxas, A low-dimensional dynamical model for the solar wind driven geotail-ionosphere system, *J. Geophys. Res.*, **103**, 4561–4572, 1998.

Iyemori, T. and D. R. K. Rao, Decay of the D_{st} field of geomagnetic disturbance after substorm onset and its implication to the storm-substorm relation, *Ann. Geophys.*, **14**, 608–618, 1996.

Kamide, Y., Is substorm occurrence a necessary condition for a magnetic storm?, *J. Geomag. Geoelectr.*, **44**, 109–117, 1992.

Kamide, Y. and N. Fukushima, Analysis of magnetic storms with DR-indices for equatorial ring current field, *Rep. Ionos. Space Res. Japan*, **25**, 125–162, 1971.

Kamide, Y., N. Yokoyama, W. Gonzalez, B. T. Tsurutani, I. A. Daglis, A. Brekke, and S. Matsuda, Two-step development of geomagnetic storms, *J. Geophys. Res.*, **103**, 6917–6921, 1998.

Klimas, A. J., D. Vassiliadis, and D. N. Baker, D_{st} index prediction using data-derived analogues of the magnetospheric dynamics, *J. Geophys. Res.*, **103**, 20,435–20,447, 1998.

Kokubun, S., Relationship of interplanetary magnetic field structure with development of substorm and storm main phase, *Planet. Space Sci.*, **20**, 1033–1049, 1972.

Kugblenu, S., S. Taguchi, and T. Okuzawa, Prediction of the geomagnetic storm associated D_{st} index using an artificial neural network algorithm, *Earth Planets Space*, **51**, 307–313, 1999.

Lundstedt, H., AI techniques in geomagnetic storm forecasting, in *Magnetic Storms, Geophys. Monogr. Ser.*, vol. 98, edited by B. T. Tsurutani, W. D. Gonzalez, Y. Kamide, and J. K. Arballo, pp. 243–252, AGU, Washington, D.C., 1997.

McPherron, R. L., The role of substorms in the generation of magnetic storms, in *Magnetic Storms, Geophys. Monogr. Ser.*, vol. 98, edited by B. T. Tsurutani *et al.*, pp. 131–148, AGU, Washington, D.C., 1997.

O'Brien, T. P. and R. L. McPherron, An empirical phase space analysis of ring current dynamics: Solar wind control of injection and decay, *J. Geophys. Res.*, **105**, 7707–7719, 2000.

Russell, C. T., R. L. McPherron, and R. K. Burton, On the cause of geomagnetic storms, *J. Geophys. Res.*, **79**, 1105–1109, 1974.

Shue, J.-H. and Y. Kamide, Effects of solar wind density on the westward electrojet, in *Substorms-4*, edited by S. Kokubun and Y. Kamide, pp. 677–680, Terra Scientific Publishing Company, Tokyo, and Kluwer Academic Publishers, Dordrecht, 1998.

Srivastava B. J., Habiba Abbas, D. R. K. Rao, and B. M. Pathan, Extended main phase of some sudden commencement great geomagnetic storms with double SSCs, *J. Atmos. Solar-Terr. Phys.*, **61**, 993–1000, 1999.

Tsurutani, B. T., W. D. Gonzalez, F. Tang, S.-I. Akasofu, and E. J. Smith, Origin of interplanetary southward magnetic fields responsible for major magnetic storms near solar maximum (1978–1979), *J. Geophys. Res.*, **93**, 8519–8531, 1988.

Vassiliadis, D., A. J. Klimas, D. N. Baker, and D. A. Roberts, A description of the solar wind-magnetosphere coupling based on nonlinear filters, *J. Geophys. Res.*, **100**, 3495–3512, 1995.

Wu, J.-G. and H. Lundstedt, Geomagnetic storm prediction from solar wind data with the use of dynamic neural networks, *J. Geophys. Res.*, **102**, 14,255–14,268, 1997.

S. Kugblenu, S. Taguchi, and T. Okuzawa (e-mail: okuzawa@ice.uec.ac.jp)